May 1998

Shear Behaviour of Railway Ballast based on Large Scale Triaxial Testing

Buddhima Indraratna
University of Wollongong, indra@uow.edu.au

D. Ionescu
University of Wollongong

H. D. Christie
Railway Services Authority of New South Wales

SHEAR BEHAVIOR OF RAILWAY BALLAST BASED ON LARGE-SCALE TRIAXIAL TESTS

By B. Indraratna,[1] Member, ASCE, D. Ionescu,[2] and H. D. Christie[3]

ABSTRACT: Quarried rock fragments (ballast) constitute one of the most commonly used construction materials in railway engineering practice. Ballast is subjected to high stress levels as well as being always exposed to environmental changes. Unsatisfactory performance of railway tracks is often associated with the loss of cross level, track profile and track alignment. The in situ condition and the engineering behavior of ballast are also important aspects governing the stability and performance of a given railway track structure. This paper presents the findings of a series of isotropically consolidated, triaxial compression tests on two modeled fractions of uniformly graded latite basalt, which is currently being used by the Railway Services Authority (RSA) of New South Wales, Australia, in the construction of new railway tracks. These tests form part of an extended research program sponsored by RSA to study the stress-strain relationships, strength properties and degradation characteristics of various types of railway ballast. The program is associated with the necessity of upgrading railway tracks for the looming Olympics in 2000. Large-scale triaxial equipment has been employed during the testing program, which is formulated to provide specific geotechnical information on the shear strength and the angle of internal friction of ballast as a function of the particle size distribution. The effect of maximum principal stress ratio on the deformation and degradation of ballast is also studied. Nonlinear relationships are developed to describe appropriately the variation of shear strength, angle of internal friction, dilation rate and degree of particle crushing at different confining pressures and principal stress ratios.

INTRODUCTION

In recent years daily congestion of highways, search for greater safety and demand for quicker intercity transport have made the railways the means of public transportation in greatest demand in New South Wales (NSW), Australia. Increased train frequency and load-carrying capacity will result in higher maintenance costs, including the consequences of ballast degradation and deformation of tracks. Worldwide, the level of funds invested in railway maintenance is substantial, and a considerable proportion of this is related to geotechnical problems. The railroads in the U.S. spend tens of millions of dollars each year for ballast and related maintenance (Chrismer 1985). In Australia, during the 1992–93 period, an excess of 1.3 million metric tons of ballast was used by the Railway Services Authority (RSA) of NSW, at a cost of over 12 million Australian dollars (Ionescu et al. 1996; H. D. Christie, personal communication, 1994). In order to reduce these costs, a proper understanding of how the ballast performs is imperative. Moreover, the exact role of the geotechnical parameters that control this performance needs thorough examination. For instance, the use of any analytical or numerical method to predict the response of railroad track to repeated wheel loading requires accurate information on the stress-strain characteristics of the component materials.

With regard to most geomaterials, the conventional triaxial apparatus is one of the most versatile and useful laboratory methods for obtaining the deformation and strength properties. In spite of its wide acceptance as the principal geotechnical apparatus for testing granular media, the disparity between the particle sizes in the field and in conventional-sized triaxial specimens can contribute to inaccurate or misleading deformation behavior and failure modes, because of the inevitable size-dependent dilation and different mechanisms of particle crushing. Therefore, the utilization of "large-scale" triaxial facilities for testing ballast becomes imperative to obtain more realistic stress-deformation and degradation characteristics. In view of the above concerns, The University of Wollongong in collaboration with the RSA of NSW has initiated a major research project on railway ballast, where both static and dynamic testing of ballast are being conducted. Only the results from the static loading tests of a latite basalt from Bombo quarry are discussed within the scope of this paper.

ROLE OF BALLAST AND NEED FOR TESTING

A conventional ballasted foundation is composed of differently graded layers of aggregates in which the sleepers (timber or concrete cross ties) are embedded. The ballast bed is required to support the applied wheel loads while preventing excessive settlement. It must also provide the necessary resiliency for the other elements of the track structure and transmit the imposed loading at an acceptable level to the foundation. Additional functions include efficient drainage of water from the ballast bed, retardation of the growth of vegetation, and providing ease of maintenance following construction (Selig and Waters 1994).

The compaction of a new or a maintained ballasted foundation is usually carried out by means of tamping and surface compaction of the crib (ballast above the level of the bottom of sleepers) and shoulders (sides of railway track). This procedure induces compaction of a rectangular column of ballast (about 200 × 300 mm) beneath the rails and the crib adjacent to the rails, whereas the surrounded ballast remains relatively uncompacted. Therefore, the most critical stage in the life of a ballasted foundation is either immediately after construction or after a maintenance cycle, when the ballast is in its loosest state, prior to being subjected to any significant traffic. It is anticipated that while the passage of trains would further compact the ballast, the applied wheel loads should prevent unacceptable breakage of particles, which could produce significant differential settlement. A major concern re-

[1]Sr. Lect., Dept. of Civ. and Min. Engrg., Univ. of Wollongong, Northfield Ave., Wollongong, New South Wales, Australia 2522; e-mail b.indraratna@uow.edu.au.

[2]Grad. Student, Dept. of Civ. and Min. Engrg., Univ. of Wollongong, Northfield Ave., Wollongong, New South Wales, Australia 2522; e-mail di02@uow.edu.au.

[3]Prin. Geotech. Engr., Geotech. Services, Railway Services Group, Railway Services Authority of New South Wales, 9-13 Unwing Bridge Rd., Sydenham, New South Wales, Australia 2044.

Note. Discussion open until October 1, 1998. To extend the closing date one month, a written request must be filed with the ASCE Manager of Journals. The manuscript for this paper was submitted for review and possible publication on March 10, 1997. This paper is part of the ***Journal of Geotechnical and Geoenvironmental Engineering***, Vol. 124, No. 5, May 1998. ©ASCE, ISSN 1090-0241/98/0005-0439–0449/$8.00 + $.50 per page. Paper No. 15318.

lating to the performance of ballast is its ability to withstand both axial and lateral forces. In practice, the effective axial stress (σ_1') and the effective lateral stress (σ_3') are related to the axle train load and the restraint provided by the sleepers and the shoulder and crib ballast. The overall effective confining stress (σ_3') is generated by the ballast's own weight at shoulders and the additional transient stress between the sleepers. When a fully loaded train passes over, the axial and lateral stresses that develop within the ballast bed are directly influenced by the initial degree of compaction. It has been demonstrated that even when a maximum static wheel load of 150 kN could treble owing to rail or wheel defects, causing high axial stresses at sleeper/ballast interfaces, the confining stress would hardly develop over 140 kN/m^2 (Raymond and Davies 1978). Consequently, of interest to the track engineer is the behavior of ballast at low confining pressures.

In the analysis and design of railway track structures, tests on scaled-down aggregates cannot be relied upon for the prediction of deformation parameters. Therefore, large-scale testing is imperative, wherein samples must be prepared according to the field grading and tested under stresses representative of the field situation. Several researchers in the past have obtained the necessary strength parameters for design from laboratory testing of large specimens on rockfill materials (Marachi et al. 1972; Marsal 1967; Charles and Watts 1980). However, it has been shown that a significant difference exists between the behavior of rockfill and railway ballast, given the distinctly different loading paths and confining pressures (Schultze 1961; Raymond et al. 1976; Selig and Alva-Hurtado 1981; Jeffs and Marich 1987). Nevertheless, past studies on railway ballast have often conducted testing at relatively high σ_3', overlooking the behavior of ballast at low σ_3'. In this paper, the shear strength, particle degradation, and dilation aspects of ballast are elucidated, with a particular reference to the effect of low confining pressures in relation to the maximum principal stress.

EXPERIMENTAL WORK

Characteristic Test on Ballast

There are four parameters that seem to be the most common contributors to the breakage of ballast, namely, hardness, toughness, particle shape, and weathering resistance (Chrismer 1985). The current standard tests for quality assessment and their recommended values represent aspects of durability, but they are not directly related to the actual performance of the track (Raymond et al. 1976). These tests generally provide basic guidelines for accepting or rejecting a given material as a potential railway ballast. Table 1 summarizes the physical properties of latite basalt used in the present study, as evaluated by the standard ballast tests ("Aggregates" 1996). On the basis of the above properties in relation to the standard recommendations and RSA specifications (Railway Services Authority 1983), one could conclude that latite basalt is a suitable ballast material having angular particles of sufficient strength. However, degradation caused by sharp edges and corners is to be expected when this material is used as ballast on a busy railway track.

TABLE 1. Characteristics of Latite Basalt

Characteristic test results (1)	Test value (2)	AS recommendations (3)
Durability		
Aggregate crushing value	12%	<25%
Los Angeles abrasion	15%	<25%
Wet attrition value	8%	<6%
Point load index	5.39 MPa	—
Crushing strength	130 MPa	—
Shape		
Flakiness	25%	<30%
Misshapen particle	20%	<30%

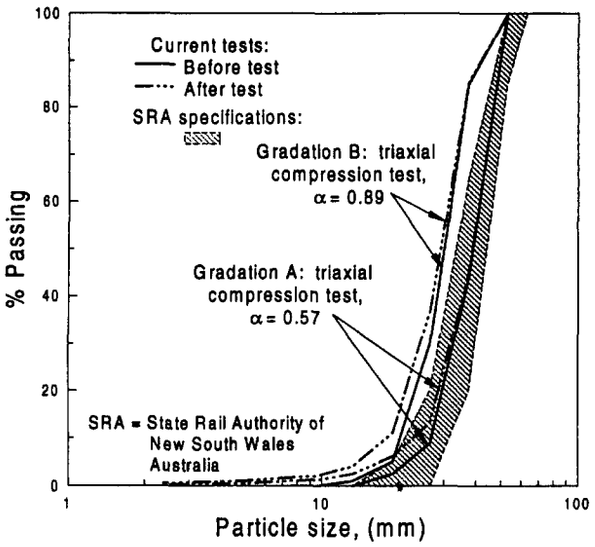

FIG. 1. Particle Size Distribution of Latite Basalt

Specimens Preparation

The latite basalt samples were obtained from a designated quarry in Bombo, Australia, having a particle size distribution representative of the actual railway ballast specified by RSA (dashed area in Fig. 1). This material has a maximum particle size just passing through the 73 mm sieve and a minimum particle size of about 13 mm. The sample size ratio is defined as the diameter of the triaxial specimen (300 mm) divided by the maximum particle dimension. It has been argued that as the sample size ratio approaches 6, the sample size effects become negligible (Marachi et al. 1972; Indraratna et al. 1993). For the tested ballast having a maximum particle dimension of 53 mm, the corresponding sample size ratio was 5.7.

The mechanical behavior of granulated materials is influenced by several factors, including the confining pressure, the porosity, and the particle size distribution. In order to determine the effect of fine particles on the overall stress-strain and degradation behavior of ballast, two separate particle gradations have been tested (Fig. 1), where the gradations A and B are parallel to the upper limit and the lower limit of RSA specifications, respectively.

Table 2 summarizes the characteristics of the laboratory

TABLE 2. Grain Size Characteristics of Latite Ballast

Test type (1)	Particle shape (2)	d_{max} (mm) (3)	d_{10} (mm) (4)	d_{30} (mm) (5)	d_{50} (mm) (6)	d_{60} (mm) (7)	C_u (8)	C_c (9)	Size ratio (10)	α (11)
Triaxial grad. A	Highly angular	53	27.1	32.6	38.9	41.3	1.5	0.9	5.7	0.57
Triaxial grad. B	Highly angular	53	20.7	26.7	30.3	32.8	1.6	1.0	5.7	0.89

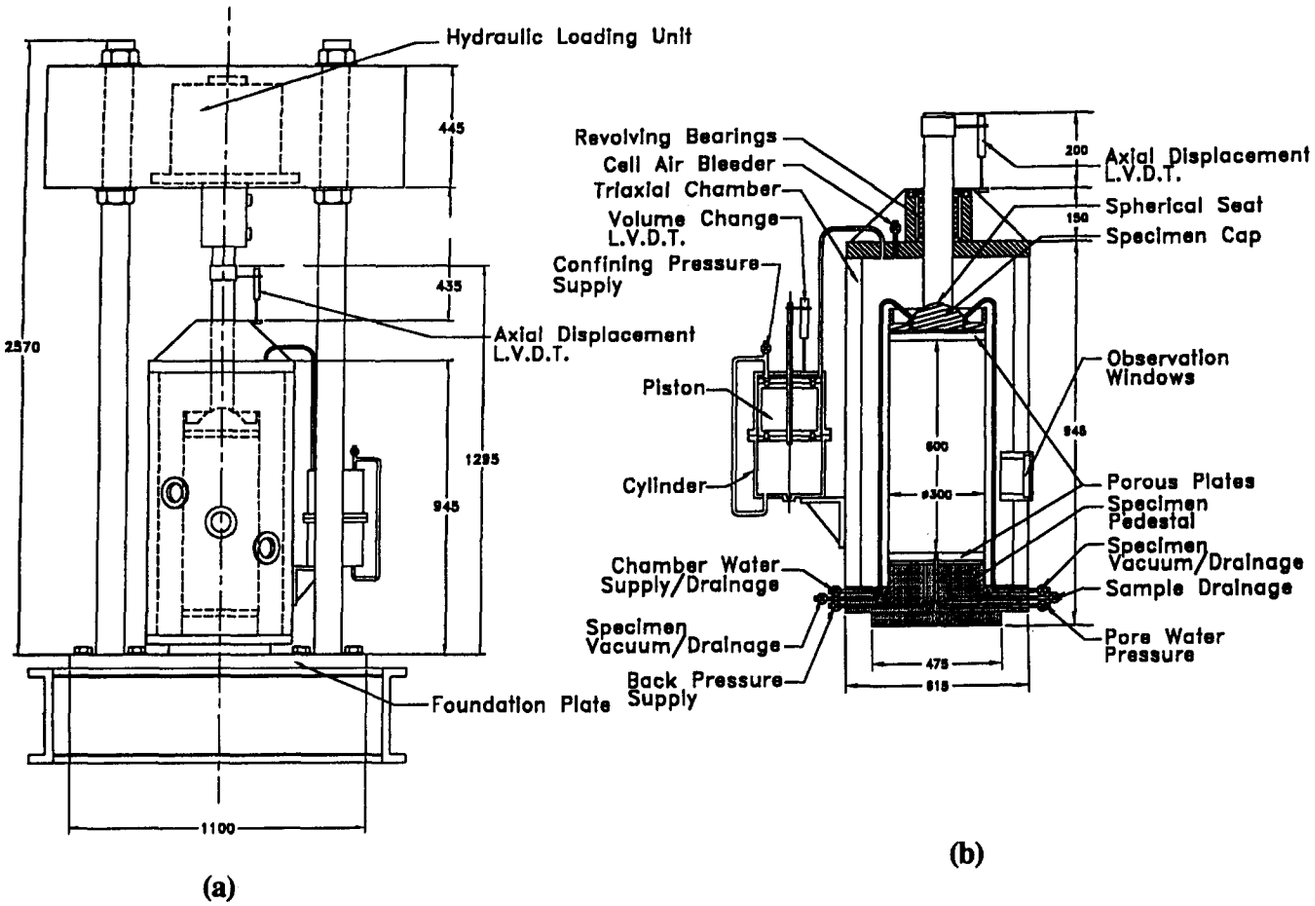

FIG. 2. Large-Scale Triaxial Equipment: (a) Schematic View of Test Frame with Triaxial Chamber; (b) Detailed Components of Triaxial Chamber

samples, including the uniformity coefficient C_u and the coefficient of curvature C_c prior to testing. The C_u value of 1.5–1.6 corresponds to a uniformly graded ballast. Apart from the conventional parameters characterizing a given particle gradation (d_{10}, d_{50}, C_u, and C_c), and additional index called the modulus of gradation (α) has been utilized to describe the particle size distribution of the specimen (Hudson and Waller 1969). This modulus of gradation (α) is a logarithmic function of the effective mean diameter of the consecutive pairs of sieves and the weight of material retained on each pair of sieves. The greater the content of fines, the higher the value of α ($\alpha = 0.57$ for gradation A and $\alpha = 0.89$ for gradation B). The ballast was compacted to simulate the realistic densities measured in the field for newly constructed tracks and those immediately after maintenance in NSW. Compaction was carried out by imparting 25 blows from a standard Proctor hammer to each layer of ballast, which had a thickness of 50–60 mm. A rubber pad (4 mm thick) was used to minimize the risk of breaking sharp corners and edges during impact. The mean bulk unit weight of the compacted specimens was determined to be 15.3 kN/m^3, which is representative of the field densities after a typical maintenance cycle. The porosity of the compacted specimens varied from 44 to 46% (D_r = 46–61%) for gradation A and from 42 to 45% (D_r = 52–63%) for gradation B.

Large-Scale Triaxial Facility

A large-scale triaxial testing apparatus (Indraratna 1996), which can accommodate specimens of 300 mm diameter × 600 mm high, was used for testing the latite ballast (Fig. 2). The apparatus consists of five main parts: the triaxial chamber, the axial loading unit, the air pressure and the water control unit, the pore pressure measurement system and the volumetric change measurement device. The axial displacement is measured by a linear variable differential transducer. A 4-mm-thick rubber membrane was used to confine the cylindrical specimens. Isotropically consolidated, drained compression tests (CID) were conducted, with the effective confining pressure varying from 1 to 240 kPa. This pressure range is adequate to simulate the typical confining pressures generated within the ballast bed by the passage of unloaded to fully loaded trains.

Compaction of specimens within the membrane was facilitated by a split cylindrical mold, which was removed before the sample was placed within the cell pressure chamber. It was verified in the laboratory that a vacuum head of 0.2 kPa was sufficient to ensure stability during the transfer of the specimen inside the triaxial cell. This small vacuum head did not cause any significant volume change of the specimen. Prior to testing, each specimen was saturated by an upward flow of water from the bottom plate. Saturation of ballast was necessary to model the deformation processes associated with "wet" ballast, especially in some of the low-lying coastal areas of NSW. Holtz and Gibbs (1956) verified that the rate of loading has little influence on shear strength measurements as long as the excess pore water pressures are kept close to zero. In this study, all tests were carried out at an axial strain rate of 0.7% per minute, allowing sufficient rate of drainage (pore pressure dissipation). The pore water pressure variation was measured using a porous disk (25 × 12 mm) attached to the bottom of specimen and connected to a pressure transducer and a digital recorder. In spite of drained conditions, very small pore pressures (less than 0.2 kPa) were occasionally observed at peak strain, but these were dissipated rapidly.

Past research has proved that even thin rubber membranes can provide some confinement, which can increase the measured principal stresses (Bishop and Henkel 1962). Considering the theory of elasticity, membrane corrections have been applied to the current stress measurements, in accordance with the procedures discussed elsewhere (Bishop and Henkel 1962; Fukushima and Tatsuoka 1984). At high pressures ($\sigma_3' > 120$ kPa), the membrane corrections amounted to less than 2% of the measured principal stresses, whereas at the lowest confining pressure ($\sigma_3' = 1$ kPa), the maximum correction was below 8%.

Each test sample was subjected to isotropic consolidation under a known (constant) cell pressure before the axial stress was increased. The volume change was monitored during consolidation and shearing in relation to the corresponding axial strain and the deviator stress. The volume change of the specimen was determined by a device (volumenometer) that consists of a piston located coaxially within a small cylindrical chamber connected to the cell. The smooth piston moves upward or downward depending on volume increase or decrease (for further detail, see Indraratna 1996). Past research has shown that if the confining pressure changes significantly during a triaxial test, the membrane penetration may introduce errors in the measurement of volume change (Bishop and Henkel 1962). However, the effect of membrane penetration is considered to be small during shearing at constant σ_3' (Charles and Watts 1980). In the current study, volume change errors caused by membrane penetration were less than 1.2%, especially as σ_3' was both constant and relatively small. The maximum deviator stress was recorded for each test specimen, and in addition the postpeak stress-strain behavior was monitored up to about 20% axial strain. In contrast to the case of sand or granulated fine media, in the case of ballast specimens no distinct failure plane was eminent even after significant postpeak straining. Therefore, for the purpose of discussion, "failure" is described by the behavior at the peak deviator stress $(\sigma_1' - \sigma_3')_p$, where the mode of failure is considered to be "bulging."

EXPERIMENTAL RESULTS AND DISCUSSION

Stress-Strain Behavior

The results of CID triaxial tests on the ballast gradations A and B are shown in Figs. 3 and 4, respectively, as plots of deviator stress, volumetric strain, and principal stress ratio against the axial strain. As expected, the peak deviator stress $(\sigma_1' - \sigma_3')_p$ increases with confining stress [Figs. 3(a) and 4(a)]. In contrast, the principal stress ratio $(\sigma_1'/\sigma_3')_p$ decreases with increasing confining pressure (σ_3') at all axial strains, as shown in Figs. 3(b) and 4(b). The postpeak response of ballast is characterized by a gradually strain-softening behavior during testing. Slightly larger principal stress ratios were obtained for gradation B, indicating the enhanced strength attributed to greater interlock of small particles in comparison with gradation A. At very low values of σ_3', both specimens exhibit volumetric dilatancy ($\varepsilon_v < 0$), whereas at higher levels of σ_3' (>120 kPa) an overall volume compression is measured for a wide range of axial strains. It is believed that the greater extent of dilation indicated by gradation B is due to the effect of denser packing of smaller particle sizes (i.e., lower void ratio at compaction).

The sample strains measured at $(\sigma_1'/\sigma_3')_p$ for different values of σ_3' are plotted in Fig. 5, where dilation (volume increase) is considered to be negative, and compression to be positive. The dilation component is plotted on the upper half of Fig. 5. The volumetric strain (ε_v) increases at a decreasing rate, with the initially dilatant behavior at low σ_3' changes to an overall compactive behavior for $\sigma_3' > 60$ kPa or so. It is not surprising that at low confining pressure ($\sigma_3' < 30$ kPa) the

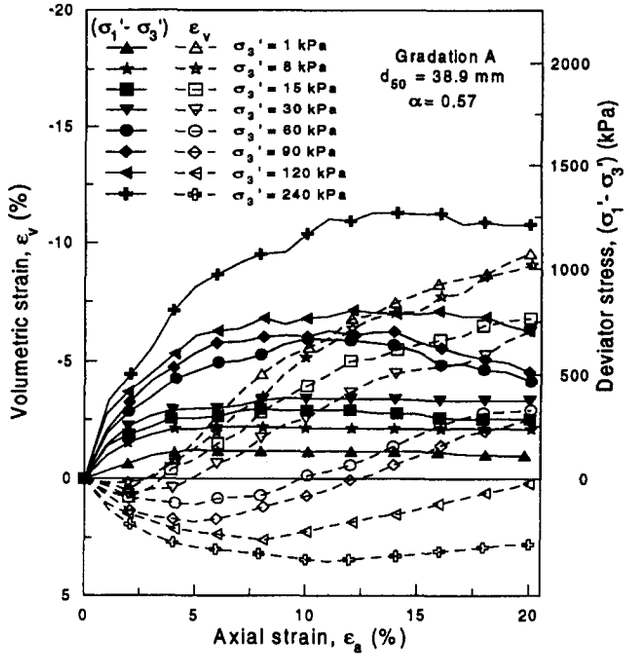

(a)

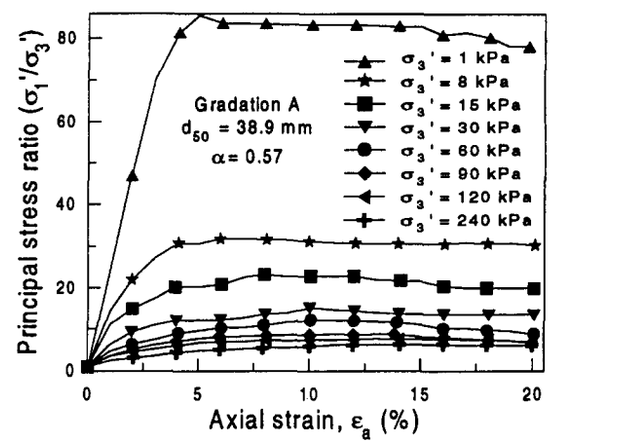

(b)

FIG. 3. Typical Stress-Strain Behavior during Triaxial Drained Compression Tests at Different Confining Pressure Values on Latite Ballast (Gradation A): (a) Variation of Deviator Stress and Volumetric Strain with Axial Strain; (b) Influence of Confining Pressure on Ratio of Principal Effective Stresses

ballast specimens exhibit significantly expansive radial strains [$\varepsilon_r = (\varepsilon_v - \varepsilon_a)/2$], thereby indicating an overall volume increase ($\varepsilon_v < 0$). However, this dilation component decreases with increasing cell pressure, and at higher levels of σ_3' the radial strain remains relatively unchanged around 5%. As expected, the axial strain at peak deviator stress increases with the confining pressure (4% at $\sigma_3' = 1$ kPa to 14% at $\sigma_3' = 240$ kPa).

The variation of the initial Poisson ratio (ν_i) and the deformation modulus [$E_i = \Delta(\sigma_1' - \sigma_3')/\Delta\varepsilon_a$] with the confining pressure is presented in Fig. 6. The initial values of ν_i and E_i have been determined for an axial strain of 2–3%. Gradation A (coarser particles) is characterized by a smaller Poisson ratio and a smaller deformation modulus. As the confining pressure exceeds 180–200 kPa, the change in ν_i and E_i is insignificant. In particular, coarser particles (gradation A) indicate a considerably greater axial strain upon initial loading (attributed to

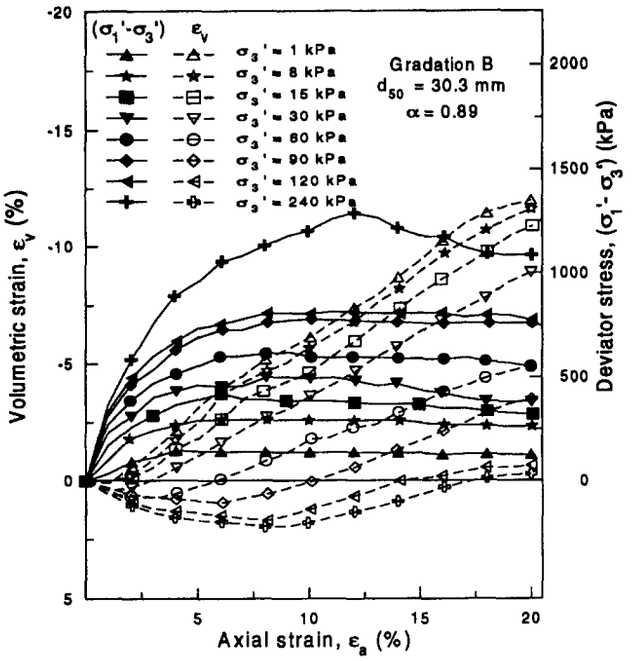

(a)

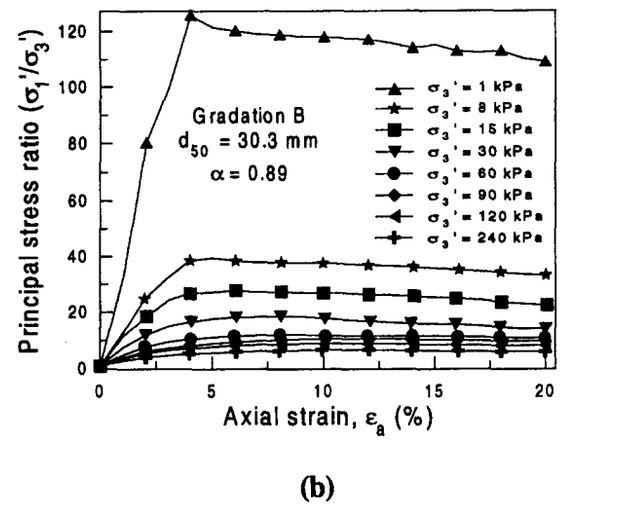

(b)

FIG. 4. Typical Stress-Strain Behavior during Triaxial Drained Compression Tests at Different Confining Pressure Values on Latite Ballast (Gradation B): (a) Variation of Deviator Stress and Volumetric Strain with Axial Strain; (b) Influence of Confining Pressure on Ratio of Principal Effective Stresses

the larger void ratio at compaction), thereby resulting in a smaller initial deformation modulus.

Shear Strength

Holtz and Gibbs (1956) have shown that, irrespective of the size of triaxial test specimens, the quarried rock fragments (angular) exhibit considerably higher shear resistance in comparison with relatively rounded river pebbles. For sandy materials, Ponce and Bell (1971) and Fukushima and Tatsuoka (1984) demonstrated that the effective principal stress ratio at failure (peak stress) increases steadily at low confining pressure ($\sigma_3' < 35$ kPa). In the same way, at low confining pressure, considerably high principal stress ratios have been observed for much larger specimens of rockfill (Marsal 1967, 1973; Marachi et al. 1972; Charles and Watts 1980). The results of the present study on latite basalt also follow the same trend as the above-mentioned granular media, as indicated in Fig. 7.

The results of various rockfill materials are also plotted for comparison. The markedly high values of maximum principal stress ratios at low confining pressure could be attributed to the greater frictional interlock of predominantly angular particles. As expected, gradation B, having a denser packing of particles, shows a higher $(\sigma_1'/\sigma_3')_p$ than gradation A. The variation of the principal stress ratio at peak stress with the confining pressure can be described by the following nonlinear relationship:

$$R_p = a(\sigma_3')^b \tag{1}$$

where R_p is the maximum principal stress ratio, a is the magnitude of $(\sigma_1'/\sigma_3')_p$ at $\sigma_3' = 1$ kPa, and b is an empirical index related to the degree of crushing or particle degradation. For the current experimental data, the following coefficients were found: for gradation A, $a = 84.98$ and $b = -0.49$, whereas for gradation B, $a = 125.17$ and $b = -0.56$ (regression coefficient $r^2 > 0.95$). These parameters are currently being used by the Railway Services Group of NSW in order to relate

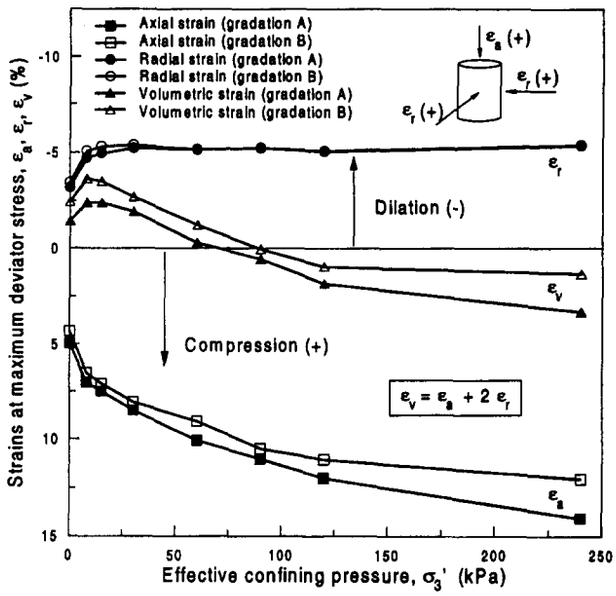

FIG. 5. Variation of Sample Strains at Peak Deviator Stress with Confining Pressure and Grain Size

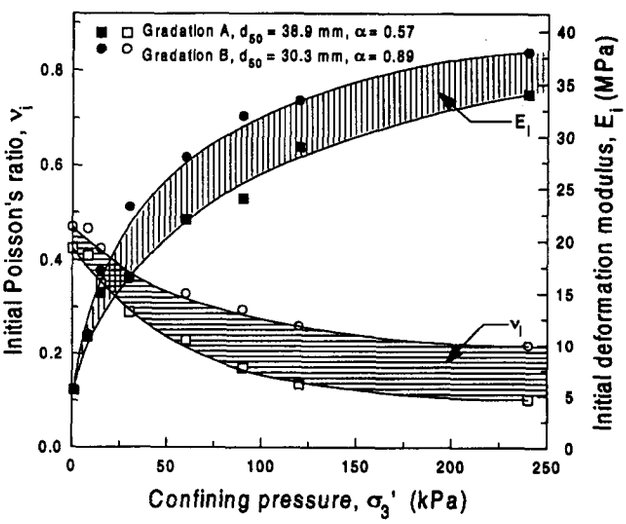

FIG. 6. Influence of Cell Pressure on Initial Deformation Modulus and Poisson's Ratio in Initial Loading Stage

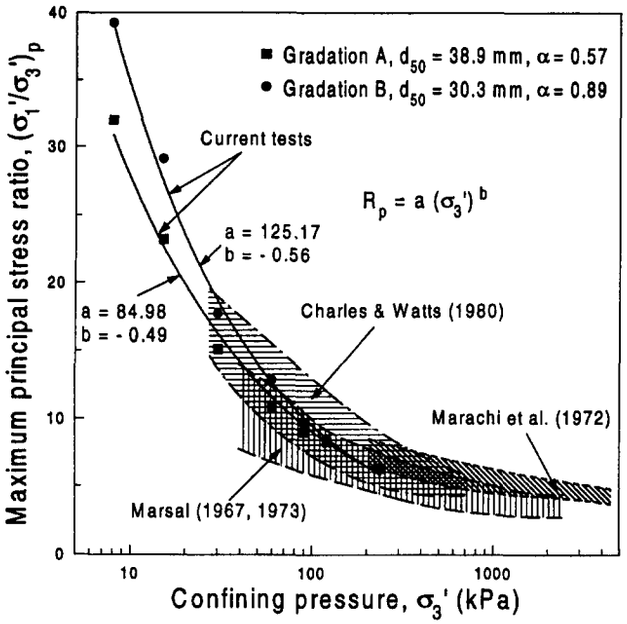

FIG. 7. Influence of Confining Pressure on Principal Stress Ratio at Peak for Basalt in Comparison with Various Granular Media (the Upper Bound of the Results from Previous Studies Representing Values Obtained on Basalt)

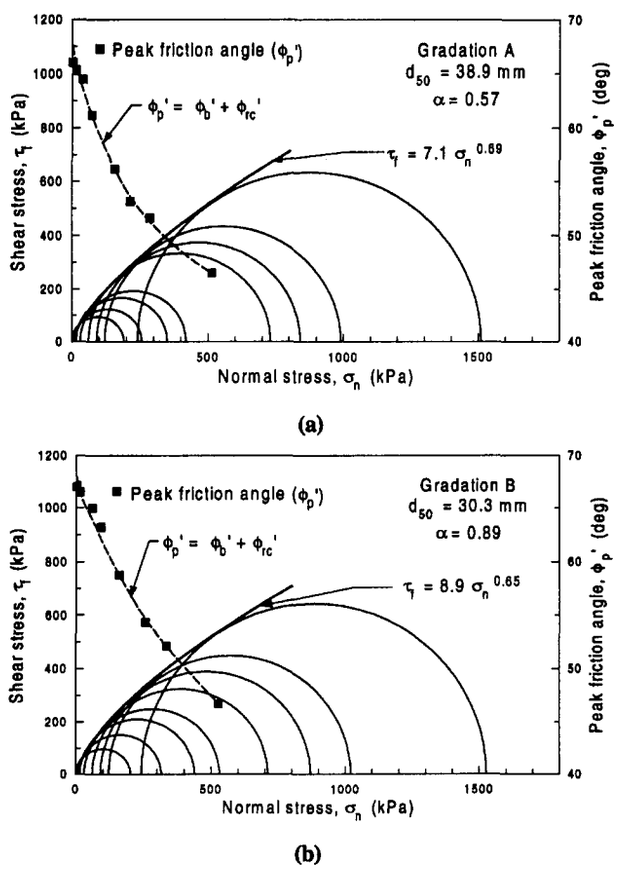

FIG. 8. Mohr-Coulomb Failure Envelopes for Latite Basalt: (a) Gradation A; (b) Gradation B

the possible ballast degradation to the critical wheel loads of full-capacity trains.

The influence of σ_3' on the shear strength of latite basalt can be represented by the conventional Mohr circles (Fig. 8). It is interesting to note that in the lower range of normal stresses, the shear strength envelope is markedly curved and passes through the origin (zero cohesion), as expected of granular materials. In fact, normal stresses below 400 kPa are usually representative of typical ballasted foundations (Jeffs and Tew 1991).

The apparent friction angle (ϕ_p') corresponding to the peak deviator stress of the ballast can be estimated by drawing a tangent from the origin to each Mohr circle of effective stresses. Its variation with the normal stress is also plotted in Fig. 8. It is important to note that, in practice, where the lateral confining stress (hence, normal stress) is usually small in railway tracks, the apparent friction angle is expected to be relatively high ($\phi_p' > 40°$). However, at large normal stress levels, the apparent friction angle becomes considerably smaller, approaching a value of the order of 35°. The change of the peak friction angle with the increase of σ_3', hence of σ_n', will be discussed in detail later.

The variation of shear strength with the increase in normal stress for basalt from different sources is presented in Fig. 9, together with the current results. All shear strength envelopes are nonlinear, especially the current test results obtained for latite basalt. The results of Charles and Watts (1980) indicate a higher shear strength, which is probably attributed to the greater unit weight (21 kN/m^3) at initial compaction, in comparison with the unit weight of current specimens (15.9 kN/m^3). At elevated normal stress, where the strength envelopes tend to become linear, the conventional (linear) Mohr-Coulomb analysis may be sufficient to describe the shear behavior. The nonlinear strength envelope is associated with the dilatant behavior of rock fragments at low normal stress.

The crushing of particles is a decisive factor in the behavior of ballast. The extent of crushing is a function of several factors, including the compressive strength of the parent rock, the applied confining pressure, and the initial compaction (porosity). Indraratna et al. (1993) proposed a nonlinear strength criterion for graywacke rockfill that was independent of the initial test conditions and was unaffected by the system of units. This criterion can be extended to describe the behavior of ballast at low confining pressure and is expressed by the following normalized relationship:

$$\tau_f/\sigma_c = m(\sigma_n/\sigma_c)^n \tag{2}$$

where σ_c is the uniaxial compressive strength of parent rock determined from the point load test, and m and n are dimen-

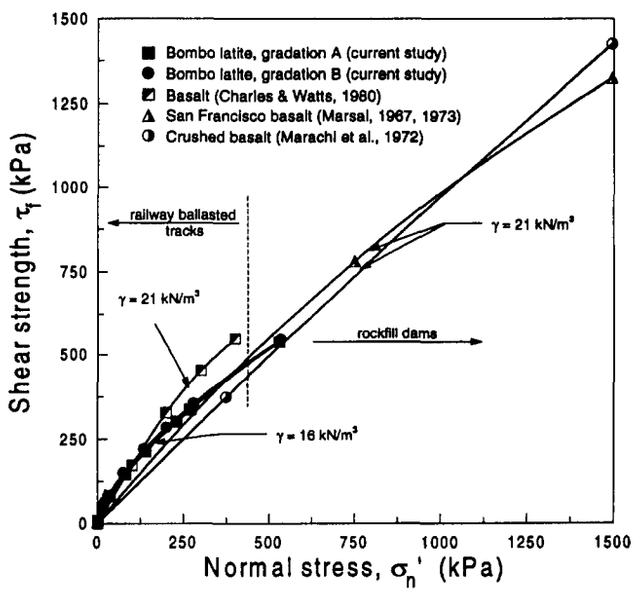

FIG. 9. Combined Data from Previous and Current Studies Representing the Shear Behavior of Basalt at a Low to Medium Range of Confining Pressures

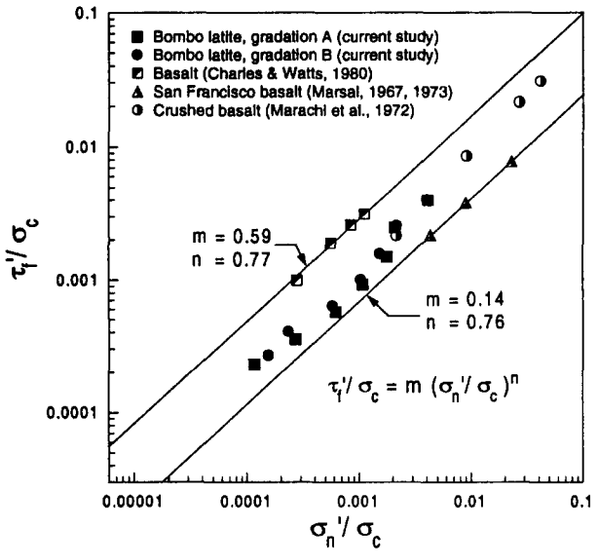

FIG. 10. Normalized Shear Strength–Normal Stress Relationship on Combined Data from Previous and Current Studies on Basalt

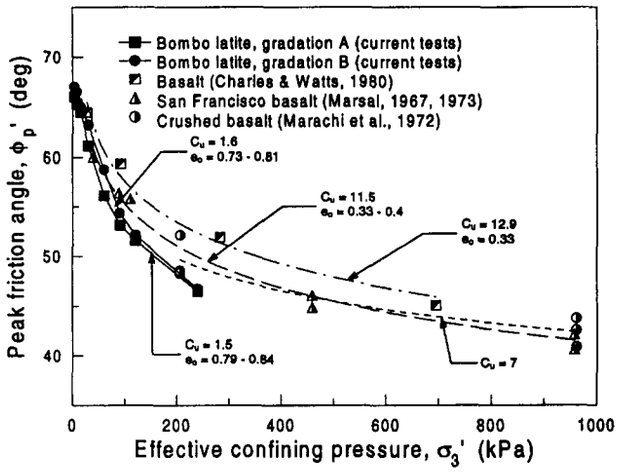

FIG. 11. Influence of Confining Pressure on the Angle of Internal Friction of Basalt at a Low to Medium Range of Confining Pressures (Combined Data from Previous and Current Studies)

sionless constants. The current experimental data in a normalized form are plotted in log scales (Fig. 10), in comparison with other results obtained for various sources of basalt. The appropriate values of m and n for these materials are summarized in Table 3. It is relevant to note that, irrespective of the compressive strength, voids ratio, particle size and distribution of these different types of basalt, all test results still fall within a narrow band, as shown in Fig. 10. It is clear from (2) that the nonlinearity of the strength envelope is governed by the coefficient n. For small confining pressures (below 200 kPa), n takes values of the order of 0.65–0.70, whereas for significantly higher levels of σ_3', the increasingly linear strength envelope is associated with n values close to or exceeding 0.8. At extremely high confining stresses (σ_3' > 2000 kPa) the magnitude of m can be estimated from the ratio of shear strength to normal stress (i.e., tan ϕ') in the event of n approaching unity. However, such levels of σ_3' are not encountered in railway tracks. The main advantage of (2) is that by knowing the uniaxial compressive strength of the parent rock, the shear strength envelope can be estimated for a given railway ballast based on the proposed m and n coefficients.

Influence of Confining Pressure on Friction Angle

It has been established that the friction angle of granular media is primarily a function of ballast gradation, particle shape, angularity, surface texture, and grain size (Holtz and Gibbs 1956; Marachi et al. 1972; Charles and Watts 1980). Bishop (1966) and Vesic and Clough (1968) confirmed that during CID tests on sand, the internal friction angle decreased as the confining pressure was increased. A number of studies on rockfill also show that the increase in confining pressure results in a decrease in the maximum principal stress ratio, with an associated reduction in the angle of friction (Marsal 1967, 1973; Charles and Watts 1980; Indraratna et al. 1993). Fig. 11 presents the variation of the drained internal friction angle ϕ_p' with the increase in confining (cell) pressure for latite basalt, together with the results from other studies on basalt. With the increase in confining pressure (hence, the normal stress), the drained friction angle has dropped from 66° to 46.5° for gradation A, and 67° to 46.8° for gradation B. A similar trend of diminishing of ϕ_p' with increasing σ_3' is also observed for basalt from other sources. However, a less uniform or better graded distribution (C_u = 12.9) having a denser packing state (e_0 = 0.33) yields larger values of ϕ_p' for similar confining pressures. At high confining pressure (>400 kPa) the reduction in ϕ_p' is not very significant, and at these levels of stress, the effects of particle sizes and their distribution become negligible. It is important to note that ballast having a narrow gradation exhibits a higher rate of decrease of ϕ_p' than rockfill materials that have broader gradations.

The high values of the apparent friction angle at low cell pressure are believed to be related to the interparticle contact forces that are well below the crushing strength of the parent rock and to the ability of the interlocking particles to dilate under lower stress levels. A number of researchers have reported similar effects for other granular media, including sand, gravel, and rockfill (Lee and Seed 1967; Feda 1971; Marsal 1973). Moreover, Charles and Watts (1980) argued that relatively strong basalt indicates a greater degree of dilatancy than

TABLE 3. Coefficients of Proposed Failure Criteria for Basalt from Different Sources

Basalt type (1)	σ_c (MPa) (2)	Initial voids ratio (3)	d_{max} (mm) (4)	d_{50} (mm) (5)	C_u (6)	Sample size (7)	σ_3' range (kPa) (8)	Coefficient	
								m (9)	n (10)
Gradation A[a]	130	0.79–0.84	53	38.9	1.6	5.7	1–240	0.18	0.69
Gradation B[a]	130	0.73–0.81	53	30.3	1.5	5.7	1–240	0.14	0.65
Crushed basalt[b]	175	—	50	13	7	6	200–4,500	0.55	0.90
San Francisco basalt[c]	175	0.33–0.41	80	7	11	5.7	400–2,470	0.14	0.76
Basalt[d]	360	0.33	38	13	13	6	30–500	0.59	0.77

[a]Present study.
[b]Marachi et al. (1972).
[c]Marsal (1967, 1973).
[d]Charles and Watts (1980).

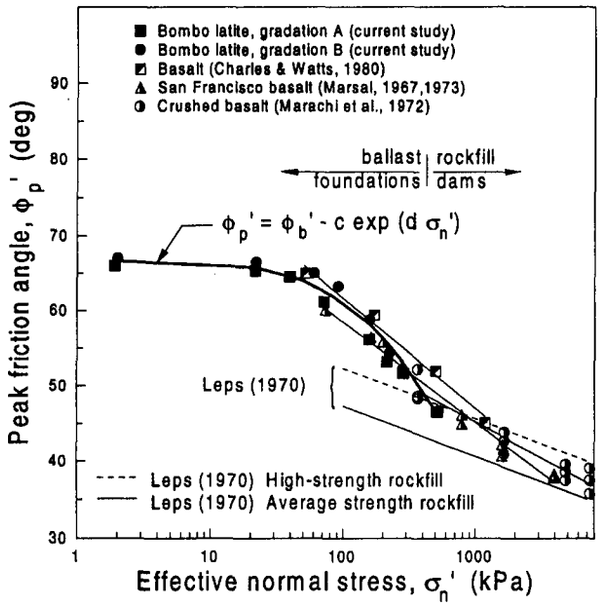

FIG. 12. Shearing Strength of Bombo Latite Basalt in Comparison with Other Basalts from Previous Studies

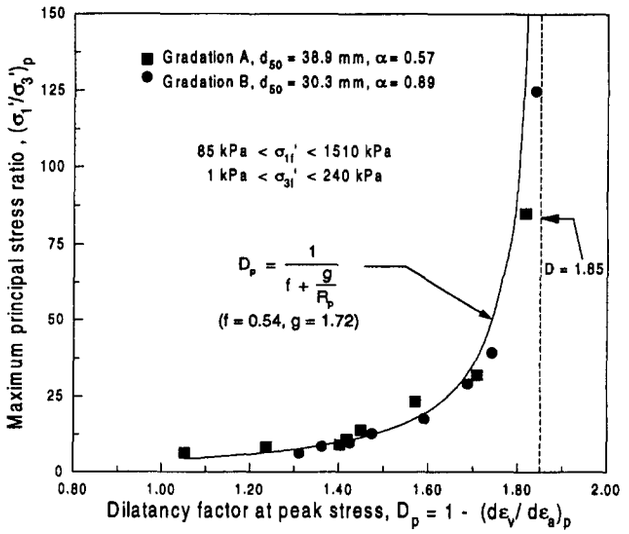

FIG. 13. Strength–Dilatancy Relationship for Bombo Basalt

the weaker rockfill media. Bolton (1986) has discussed the effect of dilation on the friction angle of sand. However, owing to the significant difference in particle sizes (between sand and ballast) and the applied range of σ_3', Bolton's equation for sands may not be applicable to ballast without considerable modification.

The effect of normal stress on the angle of friction is illustrated in Fig. 12, which includes the present data together with other results of basalt tested by Marsal (1967, 1973), Marachi et al. (1972), and Charles and Watts (1980). The shear strength limits proposed by Leps (1970) for rockfill materials are also plotted for comparison. While a slight reduction in the peak friction angle is observed for low normal stresses below 20 kPa, above this level and up to 500 kPa a small increase in normal stress induces a considerable decrease in ϕ_p'. For the appropriate normal stress range applicable for railway tracks ($\sigma_n' < 400$ kPa) the variation of ϕ_p' with σ_n' is described by the following exponential equation:

$$\phi_p' = \phi_b' + c \exp(d\sigma_n') \tag{3}$$

where ϕ_b' is the true interparticle friction angle determined from tilt table test, and c and d are empirical coefficients. The second term in (3) reflects the combined effect of particle rearrangement, dilation, and particle degradation during loading under a given normal (confining) stress. For latite basalt having a value of $\phi_b' = 35°$, the test coefficients were determined to be $c = 31.9$ and $d = -0.002$. However if (3) is expressed in terms of the mean effective stress [$p' = (\sigma_1' + 2\sigma_3')/3$], coefficients c and d are affected. For instance, for $p' < 400$ kPa, $c = 35.5$ and $d = -0.0015$. In most ballasted tracks where the lateral confining pressure is very small, σ_n' in (3) can be replaced with the axial stress applied by the wheel loading. In other words, if the friction angle of a given ballast at small confining pressures is known, the admissible axial (wheel) loads can be estimated.

Effect of Confining Pressure on Sample Deformation

Previous studies by a number of investigators have shown that the extent of volumetric deformation during shear has a significant bearing on the measured strength. It was shown earlier that at lower levels of confining pressure, the volume of particulate (granular) media can expand upon loading, and that this behavior is more pronounced for dense specimens (Raymond and Davies 1978). It has been argued that the rate of volume change at peak stress, or "failure," decreases with increasing cell pressure (Billam 1971) and that larger dilation rates ($-d\varepsilon_v/d\varepsilon_a$) have been associated with high maximum principal stress ratios (Charles and Watts 1980). Moreover, it follows that the curvature of the shear strength envelope is related to the dilation rate, particularly at small σ_3'.

The effect of maximum principal stress ratio $(\sigma_1'/\sigma_3')_p$ on the rate of dilation is illustrated in Fig. 13, where the dilatancy factor (D_p) is defined by $1-(d\varepsilon_v/d\varepsilon_a)_p$ (Rowe 1962). It is shown that the relationship between the maximum principal stress ratio and D_p is highly nonlinear for the range of applied σ_3'. Although this seems to be in contradiction with the somewhat linear variation presented by Bishop (1966) for CID triaxial tests on sand, it may be noted that Bishop's results were obtained for tests conducted at much higher confining stresses, which are not applicable to railway ballast. The nonlinear variation of the dilatancy factor with the maximum principal stress ratio becomes asymptotic to $D_p = 1.85$. For similar triaxial tests conducted on rigid granular materials by Horne (1965), the measurements indicate a dilatancy factor less than 2. By using a hyperbolic fit, the following equation is obtained to describe the relationship between the ballast dilatancy factor and the maximum principal stress ratio:

$$D_p = \frac{1}{f + g/R_p} \tag{4}$$

where D_p is the dilatancy factor at the maximum principal stress ratio, R_p is the ratio of principal stress at peak, and f and g are experimental constants. For latite basalt tested here, the experimental constants are $f = 0.54$ and $g = 1.72$.

PARTICLE BREAKAGE

The degree of particle crushing affects the deformation and the ultimate strength characteristics of any ballast material (Raymond et al. 1976; Jeffs and Marich 1991; Selig and Waters 1994), which in turn influence the track performance. Initially, local crushing at interparticle contacts takes place, followed by complete fracture of weaker particles on further increase in load. This grain breakage contributes to differential track settlement and lateral deformation. Also, the long-term accumulation of fines and decreasing porosity of ballast at certain depths can cause undrained failures during and after heavy rainfall.

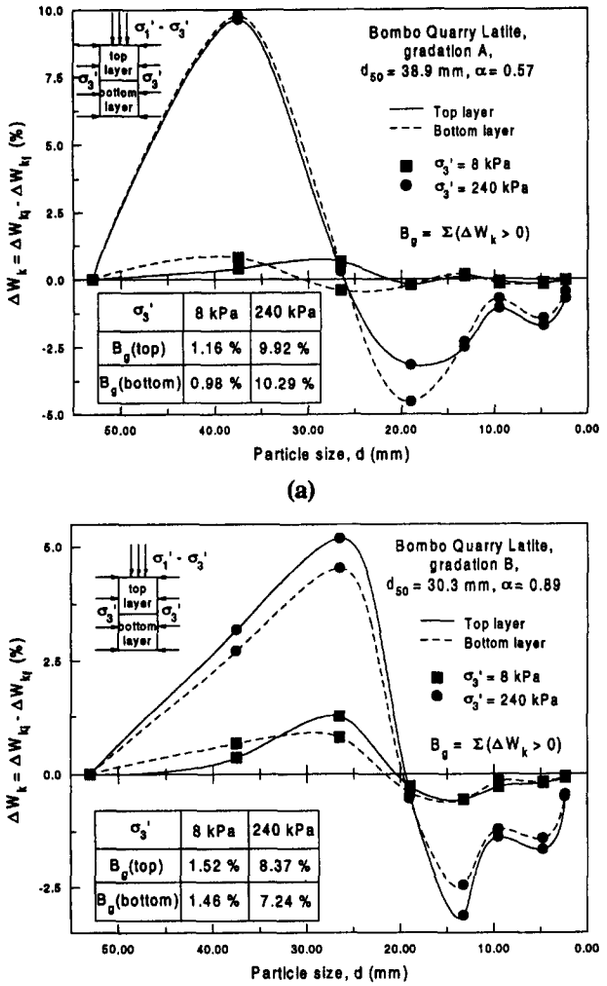

FIG. 14. Variation of Particle Distribution with Grain Size for Bombo Basalt Sheared at Different Confining Pressures, Corresponding to Each Layer of Ballast: (a) Gradation A; (b) Gradation B

TABLE 4. Particle Breakage Index for Bombo Basalt

Cell pressure (kPa) (1)	LAYER			
	Gradation A		Gradation B	
	B_g top (%) (2)	B_g bottom (%) (3)	B_g top (%) (4)	B_g bottom (%) (5)
1	1.12	0.91	1.50	1.36
8	1.16	0.98	1.52	1.46
15	1.35	1.03	2.66	2.26
30	2.07	2.01	2.39	1.99
60	3.21	3.19	4.51	4.38
90	4.51	4.73	6.27	4.99
120	6.11	6.5	8.25	6.57
240	9.92	10.2	8.37	7.24

The particle size distribution of granular materials continuously change during the loading process owing to the degradation of particles, as shown earlier in Fig. 1. In overstressed railway foundations, rapid fragmentation of the particles and the subsequent clogging of ballast voids with fines are commonly observed (Selig and Waters 1994; Ionescu et al. 1996). It has been reported that the primary cause of ballast contamination is the breakdown of aggregates (Chrismer and Read 1994), which accounts for up to 40% of "fouled" material (Selig and Waters 1994).

In order to determine the degradation characteristics of latite basalt with depth, the test specimens were divided into two equal layers (300 mm high) separated by a thin geotextile interface, which prevents the migration of pulverised particles from the top toward the bottom of the specimen. After each test, the sample was sieved and the changes in the grading were recorded for both layers. Often, the small changes in particle sizes caused by degradation cannot be clearly illustrated in conventional particle size distribution curves (Fig. 1). Therefore, as an alternative, the differences in the percentage by weight of each grain size fraction before and after the test (ΔW_k) are plotted against the aperture of the lower sieve corresponding to that fraction (Fig. 14). A measure of grain breakage (B_g) equal to the sum of the positive values of ΔW_k, expressed as a percentage, has been introduced by Marsal (1973) for granular materials. Table 4 presents the computed values of B_g for each layer of ballast gradations A and B, at different cell pressures. It is observed that, on the average, a greater extent of particle breakage occurs within the upper part of the specimen. Given that the load distribution is expected to be uniform throughout the depth of the triaxial specimen, the localized breakage of particles may be attributed to the nonuniform stress concentrations caused by the angularity (sharp corners) of ballast. The particle breakage occurs where contact stresses are maximum and often much larger than the applied deviator stress, $\sigma_1' - \sigma_3'$. The stress redistribution within a ballast specimen is very difficult to predict, especially when the angular particles are not homogeneous. It may also be possible that the geotextile could have introduced a "strain constraint," whereby the upper portion of the sample could have been subjected to a greater extent of shearing stress. As illustrated in Fig. 14, for both gradations the breakage affects mainly the larger grains (26.5–53 mm). More significantly, this degradation phenomenon is more pronounced at higher confining pressures. Smaller particles subjected to small confining stresses are the least affected by grain breakage.

Fig. 15 illustrates the variation of the particle breakage index with the change in the maximum principal stress ratio. The value of B_g was averaged over the entire length of the specimen, which varies from 0.95 to 10.1% for gradation A and from 1.3 to 7.8% for gradation B. Not surprisingly, a greater extent of degradation was observed for gradation B, owing to the greater initial density upon compaction. A nonlinear relationship between the maximum principal stress ratio and the particle breakage index is proposed:

$$R_p = h(B_g)^i \tag{5}$$

where R_p is the maximum principal stress ratio, and h and i are empirical coefficients. From the current test results, the following empirical coefficients were determined for latite basalt: for gradation A, $h = 24.10$ and $i = -0.63$, whereas for gradation B, $h = 60.88$ and $i = -1.05$. Once the average value of B_g is known for a given type of ballast, the allowable applied loads can then be estimated to prevent significant particle degradation.

Alternatively, the relationship between the friction angle and B_g can be defined as follows:

$$\phi_p' = j(B_g)^k \tag{6}$$

where j and k are empirical coefficients. For gradation A, $j = 64.84$ and $k = -0.13$, whereas for gradation B, $j = 73.19$ and $k = -0.18$. Once the friction angle is known for a given ballast, the corresponding particle breakage index and, hence, the maximum principal stress ratio can then be estimated using (5) and (6), as illustrated diagrammatically in Fig. 15.

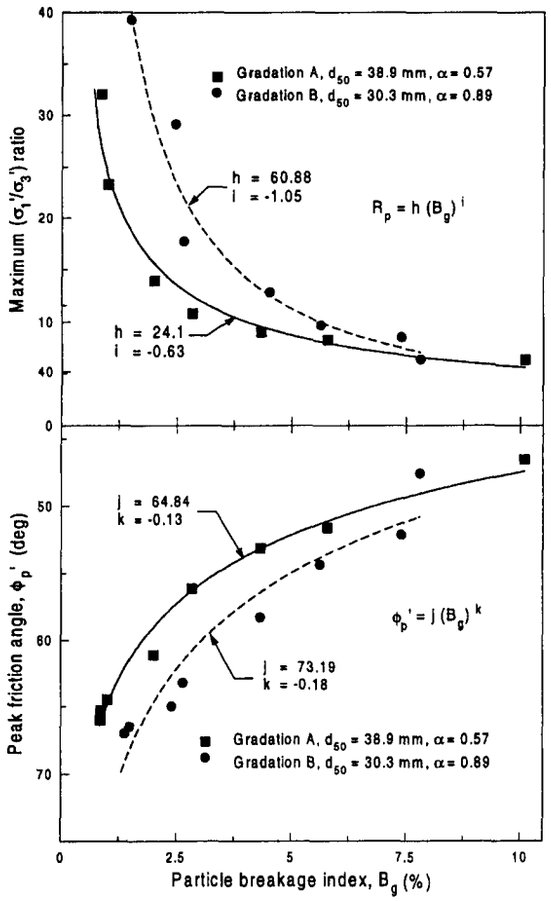

FIG. 15. Effect of Stress Variation on Particle Breakage for Bombo Basalt

CONCLUSIONS

The investigations covered herein verify that the deformation and shear behavior of latite basalt at low levels of confining pressure (<100 kPa) depart significantly from the behavior at larger confining pressure. The shear strength and the crushing of particles are mainly influenced by the particle size distribution, the angularity of grains, and the degree of packing (initial density). It is anticipated that ballast with a broader gradation that is densely compacted will undergo a greater degree of degradation upon loading. Naturally, the greater the rate of "fouling" the higher the cost of maintenance.

The angle of internal friction is a function of the confining pressure, where pronounced nonlinearity of the strength envelope is evident at $\sigma_3' < 100$ kPa. The initial deformation modulus can be increased substantially by a less than proportional increase in the confining pressure, especially at the lower stress range (1–100 kPa). This suggests the importance of efficient track maintenance by ensuring a full and compacted crib between the sleepers and high shoulders at all times. The current study has introduced a modified shear strength criterion for ballast at appropriate levels of confining pressure (<240 kPa in the laboratory). This strength criterion incorporates the (uniaxial) compressive strength of the parent rock. In the absence of detailed experiments, this strength criterion can still be used for preliminary design.

Experimental data have also shown that the enhanced dilatant behavior of ballast during shearing at low σ_3' is associated with an increase in the maximum principal stress ratio. Moreover, the rate of dilatancy is related to the degree of particle degradation. At high σ_3' values where dilation is suppressed, the breakage index, B_g, increases substantially. Although the applied stresses in a triaxial cell are uniform, the laboratory results indicated that a greater degree of particle crushing occurred within the top part of the ballast specimen. It is difficult to predict the degradation mechanisms of ballast upon loading, mainly because of its highly inhomogeneous nature. The breakage of ballast is a function not only of the applied deviator stress and confining pressure; it is also related to the excessive contact stresses generated within the body of angular particles. In the field, greater axial stresses near the surface tend to cause significant breakage of ballast just beneath the sleepers. Also, the confining pressures are never uniform with depth in the track. Considering the two different stress states in the laboratory and in the field, it is difficult to extrapolate directly the particle degradation data obtained in the triaxial chamber to the field situations.

The CID triaxial test results provide valuable information on the stress-strain behavior and the degradation characteristics of a typical ballast (latite basalt) under static loading conditions. However, the static tests alone do not model the field situation completely, because the speed and frequency of trains impart a quasi-cyclic load on the ballasted foundation, generating nonuniform vibrations that affect particle behavior in a dynamic sense. In the light of this, dynamic, cubical triaxial tests are now being conducted by the writers, and these results will be published at a later stage upon completion of this experimental phase.

APPENDIX I. REFERENCES

"Aggregates and rock for engineering purposes." (1996). *AS 2758.7-96*, Standards Australia, Sydney, NSW, Australia.

Billam, J. (1971). "Some aspects of the behaviour of granular materials at high pressures." *Proc., Roscoe Mem. Symp.*, Whitefriars Press Ltd., London, U.K., 69–80.

Bishop, W. A. (1966). "The strength of soils as engineering materials." *Géotechnique*, London, U.K., 16(2), 91–129.

Bishop, W. A., and Henkel, D. J. (1962). *The measurement of soils properties in the triaxial test.* Edward Arnold Ltd., London, U.K.

Bolton, M. D. (1986). "The strength and dilatancy of sand." *Géotechnique*, London, U.K., 13(1), 65–78.

Charles, J. A., and Watts, K. S. (1980). "The influence of confining pressure on the shear strength of compacted rockfill." *Géotechnique*, London, U.K., 30(4), 353–367.

Chrismer, S. M. (1985). "Considerations of factors affecting ballast performance." *Rep. No. WP-110, Administration of American Railroads, Research and Test Department, Bulletin 704*, Am. Railway Engrg. Assn.

Chrismer, S. M., and Read, D. M. (1994). "Examining ballast and subgrade conditions." *Railway Track and Struct.*, June, 39–42.

Feda, J. (1971). "The effect of grain crushing on the peak angle of internal friction of a sand." *Proc., 4th Conf. on Soil Mech.*, Hungarian Academy of Science, Budapest, 79–93.

Fukushima, S., and Tatsuoka, F. (1984). "Strength and deformation characteristics of saturated sand at extremely low pressures." *Soils and Found.* Tokyo, Japan, 24(4), 30–48.

Holtz, W. G., and Gibbs, H. J. (1956). "Triaxial shear tests on pervious gravely soils." *J. Soil Mech. and Found. Div.*, ASCE, 82(1), 1–22.

Horne, M. R. (1965). "The behaviour of an assembly of round, rigid cohesionless particles." *Proc., Roy. Soc.*, London, U.K., A286, 62–97.

Hudson, S. B., and Waller, H. F. (1969). "Evaluation of construction control procedures-aggregate gradation variations and effects." *Rep. No. 69*, National Co-Operative Highway Research Program.

Indraratna, B. (1996). "Large-scale triaxial facility for testing non-homogeneous materials including rockfill and railway ballast." *Australian Geomechanics*, Australia, 30, 125–126.

Indraratna, B., Wijewardena, L. S. S., and Balasubramaniam, A. S. (1993). "Large-scale triaxial testing of greywacke rockfill." *Géotechnique*, London, U.K., 43(1), 37–51.

Ionescu, D., Indraratna, B., and Christie, D. (1996). "Laboratory evaluation of the behaviour of railway ballast under static and repeated loads." *Proc., 7th Australia New Zealand Conf. on Geomech.*, Inst. of Engrg., Adelaide, Australia, 86–91.

Jeffs, T., and Marich, S. (1987). "Ballast characteristics in the labora-

tory." *Proc., Conf. Railway Engrg.*, Inst. of Engineers, Perth, Australia, 141–147.
Jeffs, T., and Tew, G. P. (1991). *A review of track design procedures—Sleepers and ballast*, vol 2 of *Railways of Australia*, Melbourne, Australia.
Lee, K. L., and Seed, H. B. (1967). "Drained strength characteristics of sands." *J. Soil Mech. and Found. Div.*, ASCE, 93(6), 117–141.
Leps, T. M. (1970). "Review of shearing strength of rockfill." *J. Soil Mech. and Found. Div.*, ASCE, 96(6), 1159–1170.
Marachi, N. D., Chan, C. K., and Seed, H. B. (1972). "Evaluation of properties of rockfill materials." *J. Soil Mech. and Found. Div.*, ASCE, 98, 95–114.
Marsal, R. J. (1967). "Large scale testing of rockfill materials." *J. Soil Mech. and Found. Div.*, ASCE, 93(2), 27–43.
Marsal, R. J. (1973). "Mechanical properties of rockfill." *Embankment dam engineering*. Wiley, New York, 109–200.
Ponce, M., and Bell, J. M. (1971). "Shear strength of sand at extremely low pressures." *J. Soil Mech. and Found. Div.*, ASCE, 97(4), 625–638.
Raymond, G. P., and Davies, J. R. (1978). "Triaxial test on dolomite railroad ballast." *J. Soil Mech. and Found. Div.*, ASCE, 104(6), 737–751.
Raymond, G. P., Lake, R. W., and Boon, C. J. (1976). "Stresses and deformations in railway track." *CIGGT, Rep. No. 76-11*, Canadian Inst. of Guided Ground Transport, Queen's University Press, Ontario, Canada.
Rowe, P. W. (1962). "The stress-dilatancy relation for static equilibrium of an assembly of particles in contact." *Proc., Roy. Soc.*, London, U.K., A 269, 500–527.
Schultze, E. (1961). "Elastic properties of ballast." *Proc., 5th Int. Conf. on Soil Mech. and Found. Engrg.*, Dunod Publishers, Paris, France, 323–327.
Selig, E. T., and Alva-Hurtado, J. E. (1981). "Permanent strain behaviour of railroad ballast." *Proc., 10th Int. Conf. Soil Mech. and Found. Engrg.*, Pergamon Press, New York, 543–546.
Selig, E. T., and Waters, J. M. (1994). *Track geotechnology and substructure management*. Thomas Telford Services Ltd., London, U.K.
Railway Services Authority of NSW. (1983). "Specification for supply of aggregate for ballast." *T.S. 3402–83*, Way and Works Branch, State Rail Authority of NSW, Sydney, Australia.
Vesic, A. S., and Clough, G. W. (1968). "Behavior of granular materials under high stresses." *J. Soil Mech. and Found. Div.*, ASCE, 94(3), 661–688.

APPENDIX II. NOTATION

The following symbols are used in this paper:

a = coefficient;
B_g = grain breakage index;
b = coefficient;
c = coefficient;
D_p = dilatancy factor at peak principal stress ratio;
d = coefficient;
f = coefficient;
g = coefficient;
h = coefficient;
i = coefficient;
j = coefficient;
k = coefficient;
m = coefficient;
n = coefficient;
p' = mean normal stress;
R_p = maximum principal stress ratio $(\sigma_1'/\sigma_3')_p$;
α = modulus of gradation;
ϕ_p' = peak friction angle;
ϕ_b' = true interparticle friction angle;
σ_1' = effective major principal (axial) stress;
σ_3' = effective minor principal (confining) stress;
$(\sigma_1' - \sigma_3')_p$ = peak deviator stress;
σ_c = uniaxial compressive strength of parent rock;
σ_n' = effective normal stress; and
τ_f = shear strength.

Subscripts

b = base;
f = failure;
g = grains;
n = normal;
p = peak; and
1, 3 = principal stresses.